ADVANCED MATERIALS

Supporting Information

for *Adv. Mater.,* DOI: 10.1002/adma.202207993

Radiative Recombination Processes in Halide Perovskites Observed by Light Emission Voltage Modulated Spectroscopy

Rafael S. Sánchez, Alexis Villanueva-Antolí, Agustín Bou, Marta Ruiz-Murillo, Iván Mora-Seró, and Juan Bisquert**

Supporting Information

Radiative Recombination Processes in Halide Perovskites Observed by Light Emission Voltage Modulated Spectroscopy

Rafael S. Sánchez*[1], Alexis Villanueva-Antolí[1], Agustín Bou[1], Marta Ruiz-Murillo[2], Iván Mora-Seró[1], Juan Bisquert*[1]

[1] Institute of Advanced Materials (INAM), Universitat Jaume I, 12006 Castelló, Spain.

[2] IoTsens, 12003, Castelló, Spain.

Corresponding authors (rasanche@uji.es , bisquert@uji.es)

1. Materials and procedures

All the compounds, materials and solvents used for the synthesis of the $CsPbBr_3$ nanoparticles, as well as for the fabrication of the LEDs were employed as received from their corresponding provider companies without any further purification. Next, a list of the chemicals used for the synthesis of $CsPbBr_3$ nanoparticles: $PbBr_2$ (ABCR, 99.999%), Cs_2CO_3 (Sigma-Aldrich, 99.995%), 1-Octadecene (ODE, Sigma-Aldrich, 90%), Oleic Acid (OA, Sigma-Aldrich, 90%), Oleylamine (OLEA, Sigma-Aldrich, 70%), Hexane (Sigma-Aldrich, 99%), Methyl Acetate (MeOAc, Sigma-Aldrich, 99.5%). The LEDs were fabricated with the following materials: ITO substrates (20x20 mm, 20 $Ohm \cdot Sq^{-1}$), PEDOT:PSS (Heraeus Clevios AI 4083), Poly(N,N'-bis-4-butylphenyl-N,N'-bisphenyl)benzidine (poly-TPD, Lumtec, 97%), (1,3,5-Triazine-2,4,6-triyl)tris(benzene-3,1-diyl) tris(diphenylphosphine oxide), 2,4,6-Tris[3-(diphenylphosphinyl)phenyl]-1,3,5-triazine (PO-T2T, Lumtec, 99%), Lithium Fluoride (LiF, Sigma-aldrich), Aluminum (Lesker, 99.99%, pellets), encapsulating photocurable glue (Lumtec LT-U001) and glass cover slides (thermo scientific MENZBC080080A120).

-Synthesis and purification of $CsPbBr_3$ nanoparticles: cesium carbonate (Cs_2CO_3, 0.407g, 1.25 mmol) and oleic acid (OA, 1.25 ml, 3.5 mmol) were loaded into a 50 ml three-necked flask with octadecene (ODE, 20 ml) and heated at 120 ºC under for 1 hour in vacuum. Then, the flask atmosphere was refilled with nitrogen and the temperature of the mixture was increased to 150 ºC until the complete dissolution of cesium carbonate. Separately, a 100 ml three-necked flask was loaded with lead bromide ($PbBr_2$, 0.345g, 0.94 mmol), oleic acid (OA, 2.5 ml, 7.1 mmol) and oleylamine (OLEA, 2.5 ml, 5.3 mmol) with octadecene (ODE, 25 ml). The mixture was dried for 1h at 120ºC in vacuum and then, the flask was refilled with nitrogen and the temperature was raised to 170ºC until a clear solution was obtained. Next, 2 ml of cesium precursor solution was swiftly injected and after 5 seconds, the flask was immersed into an ice-water bath to stop the reaction. The crude was centrifuged (5000 rpm, 5 min); the supernatant was discarded and the precipitate was dispersed in hexane (5 ml). Then, MeOAc (5 ml) was added to the dispersion and a second centrifugation was carried out (5000 rpm, 5 min); again, the supernatant was discarded and the solid was redispersed in hexane (1 ml). At this point,

the dispersion was stored in an Eppendorf vial at low temperature (-18 ºC) overnight and carefully decanted to remove the solid sediment deposited at the bottom. Then, the dispersion was transferred to glass vial, dried with a gentle nitrogen flow and introduced in vacuum for 15 minutes to obtain the $CsPbBr_3$ nanoparticles as a solid. Finally, the solid was weighted (60-70 mg were typically obtained), redispersed in the corresponding volume of hexane (typically 6-7 ml) to obtain a concentration of 10 $mg \cdot ml^{-1}$, and filtered through a 0.42 µm Teflon filter for device's fabrication. UV-Vis light absorption and PL measurements were carried out to characterize the $CsPbBr_3$ colloidal dispersions.

-Fabrication of LEDs: a layer of PEDOT:PSS was deposited by spin-coating (3000 rpm, 30 seconds) on the ITO substrate, followed by a first annealing treatment at 80 ºC during 10 minutes and a second annealing at 120ºC for 10 minutes. After that, a solution of Poly-TPD (6 $mg \cdot ml^{-1}$ in Chlorobenzene) was deposited by spin-coating (3000 rpm, 30 seconds) in inert atmosphere inside a glovebox and annealed following the same procedure than in the previous step. Next, the $CsPbBr_3$ nanoparticles were deposited by spin-coating (3000 rpm, 30s) in inert atmosphere and transferred into the thermal evaporator chamber. Then, a sequential evaporation of PO-T2T (40 nm) and LiF (1 nm) layers was performed over the entire substrate area, and the aluminium contacts (100 nm) were subsequently deposited, under high vacuum conditions, using a shadow mask that consisted of 4 active areas (0.08 cm^2 each). Finally, the back contacts were covered with a photocurable glue (Lumtec LT-U001) and a glass cover slide to encapsulate the active areas upon exposure to UV-light (4 min).

-Optical characterization of $CsPbBr_3$ nanoparticles: the UV-Vis absorption spectrum of the nanoparticles in solution was acquired with a spectrophotometer (Varian Cary 300 BIO). The photoluminescence (PL) spectra and PL quantum yields (PLQY) of the $CsPbBr_3$ nanoparticles in solution were measured with an absolute PL quantum yield spectrometer (Hamamatsu C9920-02).

-Electro-optical characterization of LEDs: the performance of the LEDs and the characteristics of the emitted light were measured with an external quantum efficiency (EQE) measurement system (Hamamatsu C9920-12). The steady-state EL measurements at constant current or voltage were performed by using a potentiostat (GAMRY Reference 3000) for electrical stimulation synchronized to a CCD detector (Andor-iDUS DV420A-OE) and spectrograph (Kymera-193I-B2) setup for optical detection. For the low temperature measurements, an electro-optical probe stage (INSTEC HCP422VP) equipped with the peripheric instruments for automated control of temperature of samples was used (available temperature window from -190ºC to 400ºC).

-Light emission voltage-modulated spectroscopy: LEVS measurements were performed by inserting the LEDs into a homemade 3D-printed holder equipped with electrical probes connected to a wavefunction generator (model, brand) and applying a sinusoidal AC perturbation (±20 mV) over a DC voltage (3 to 5 V) to power the devices.

For LEVS at low temperature, the same probe stage (INSTEC HCP422VP) was used. The output light was collected by a series of collimating lenses to guide the optical signal towards a Silicon switchable gain detector (Thorlabs PDA36A2) set to 40 dB gain level, which was connected to an oscilloscope (Tektronix model) for data acquisition using the 1 MOhm input port (see the setup diagram in Fig. S7). Upon acquiring the input (modulated voltage) and output (emitted light) signals at different frequencies (from 100 mHz to 100 KHz, 5 points per decade), respectively, the data were automated translated into polar coordinates by using a Pycharm script and represented in the complex plane (S'' *vs* S'). A commercially available blue-emitting device (Thorlabs LED430L, λ_{max}= 430 nm, 8 mW) was acquired for the sake of comparison with our perovskite-based LEDs. Check supplier website for further details of the device LED430L (https://www.thorlabs.com/thorproduct.cfm?partnumber=LED430L). Note that our LEVS measurements do not provide absolute values of the photon flux emitted by the LEDs, since not all the photons are being collected by the detector, and therefore, the obtained S' and S'' values do not provide information about the absolute performance of the light-emitting devices; here, only the shapes of the S'' *vs* S' spectra are considered. Refinement of experimental setup for absolute values is under development. It is worth mentioning that the Si detector employed (PDA36A2) shows a linear response to the incident optical power, according to the formula $V_{OUT} = R_{(\lambda)} * G * S\mathrm{F} * Input\ Power\ (W)$, where $R_{(\lambda)}$ stands for its responsivity at each wavelength, G for the transimpedance gain factor selected (0-70 dB), SF a scale factor characteristic of the detector at the selected gain level and the $Input\ Power$ for the optical power emitted by the LED; therefore, if the measuring conditions are maintained, including device orientation, distance, etc., those results obtained from different devices allow relatively quantifying the device's efficiencies and the capacitive/inductive loses. Additionally, because the input and output signals collected in our measurements have the same physical units, *i.e.* electric potential, S' and S'' correspond to dimensionless magnitudes; that is the reason why all our plots of the S function in the complex plane for the different devices do not display units. If the absolute emitted photon flux had been measured, it might have been transformed into electric current units and thus the LEVS transfer function S would have admittance units (Ω^{-1}).

2. Optical characterization of $CsPbBr_3$ nanoparticles and electro-optical characterization of LEDs

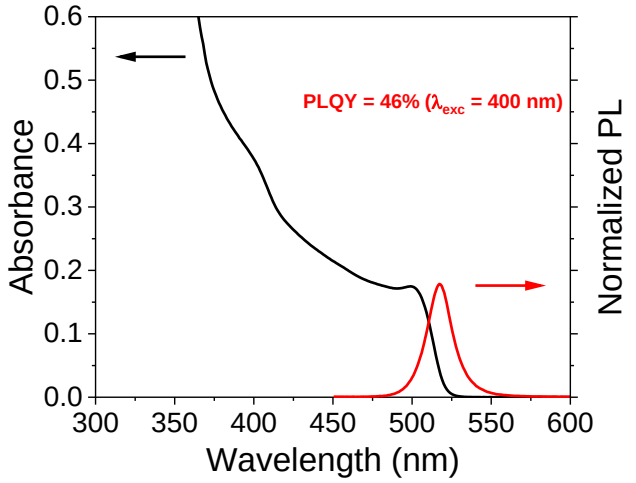

Figure S1. UV-Vis absorption and PL spectra in solution (hexane) with the PLQY value (λ_{exc} = 400 nm). The concentration of the $CsPbBr_3$ dispersion was $6.62 \cdot 10^{-2}$ mg·ml^{-1} for the determination of the absorption spectrum, whereas for the PL measurements ($\boldsymbol{\lambda_{max}^{PL}}$ = 517 nm; FWHM= 19 nm), the absorbance of the dispersion was adjusted to 0.05 units at the excitation wavelength.

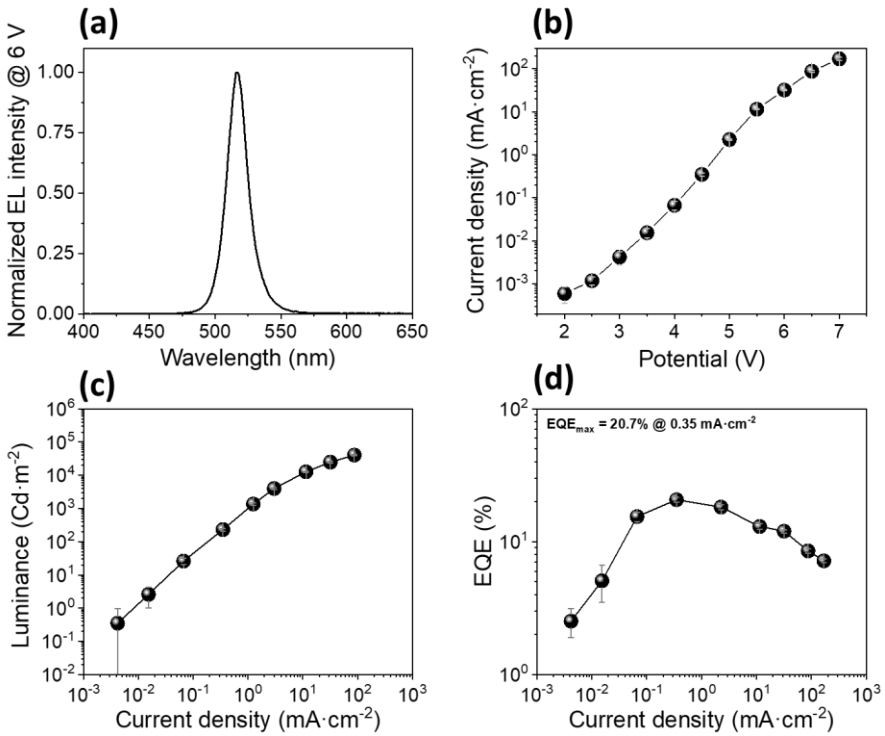

Figure S2. Electro-optical characterization of the as-made $CsPbBr_3$ LEDs: (a) EL spectrum registered at 6V ($\boldsymbol{\lambda_{max}^{EL}}$ = 517 nm; FWHM= 18 nm); (b) current density *vs* applied potential (I/V curve); (c) luminance *vs* current density; (d) external quantum efficiency (EQE) *vs* current density. The plotted current density, luminance and EQE values correspond to those averaged values obtained from more than twenty different active areas of different replicated devices, whose standard deviations are reflected by the error bars at each indicated voltage (or current density). Note that for high current densities, the luminance and EQE

error bars are smaller than the symbols themselves used to represent the averaged values.

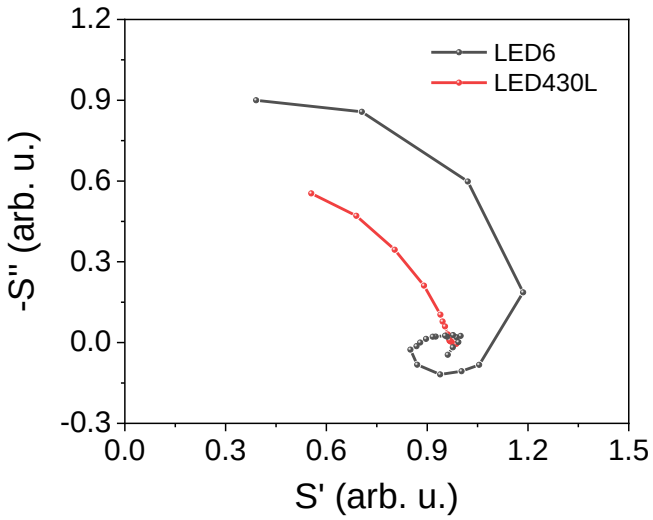

Figure S3. Representation of the S function in the complex plane (arbitrary units) of the LED6 at 4V DC ±20 mV AC, and that of a commercially available blue emitting device (LED430L) at 3V DC ±20 mV AC. Note that the actual $\boldsymbol{S'}$ and $\boldsymbol{S''}$ values registered for both devices lie in significantly different ranges; with the aim of allowing a fair comparison of the spectra's shapes, they have been multiplied by a factor to make them appear in a scale close to 1. The $CsPbBr_3$ device (LED6) displays a strong inductive component (loop in black curve) at the low frequency region, whereas LED430L (red curve) does not show it, which illustrates the characteristic behavior of the perovskite-based devices.

3. Estimation of radiative lifetime

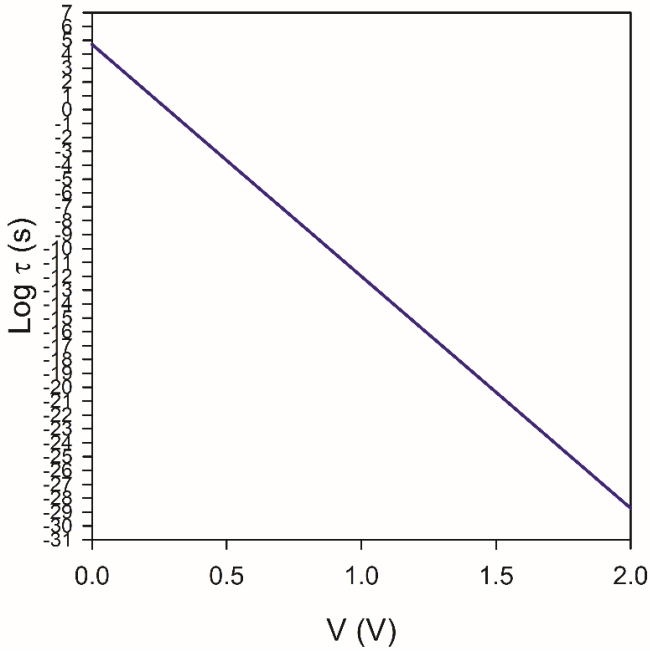

Figure S4. Calculation of $\tau_{rad} = \frac{1}{2B_{rad}n_i} e^{-qV/k_BT}$ using $B_{rad} = 1x10^{-10}$ cm^{3}s^{-1}, $n_i = 1x10^5$ cm^{-3} values from literature: Wolff, C. M. *et al.*, *Adv. Energy Mater.* **2021**, *11*, 2101823 and Krückemeier, L. *et al.*, *Adv. Energy Mater.* **2021**, *11*, 2102290.

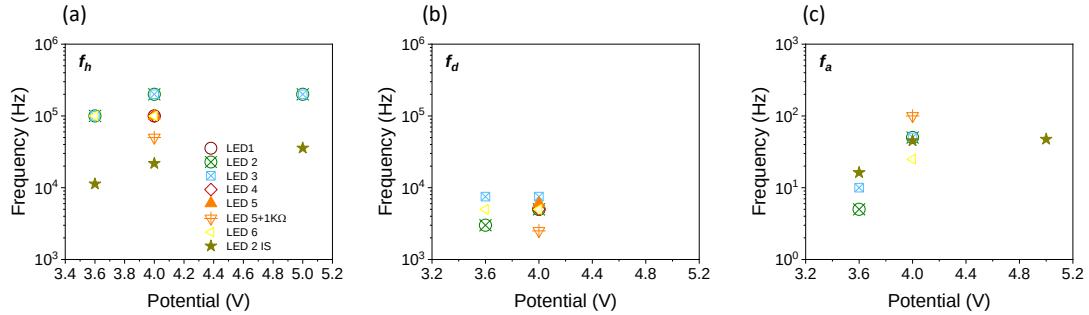

Figure S5. Experimental characteristic frequencies obtained by LEVS (color points) and impedance spectroscopy (star points), for different devices according to the model of Fig. 7c, (a) high frequencies and (b-c) low frequencies.

4. Effect of the series resistance

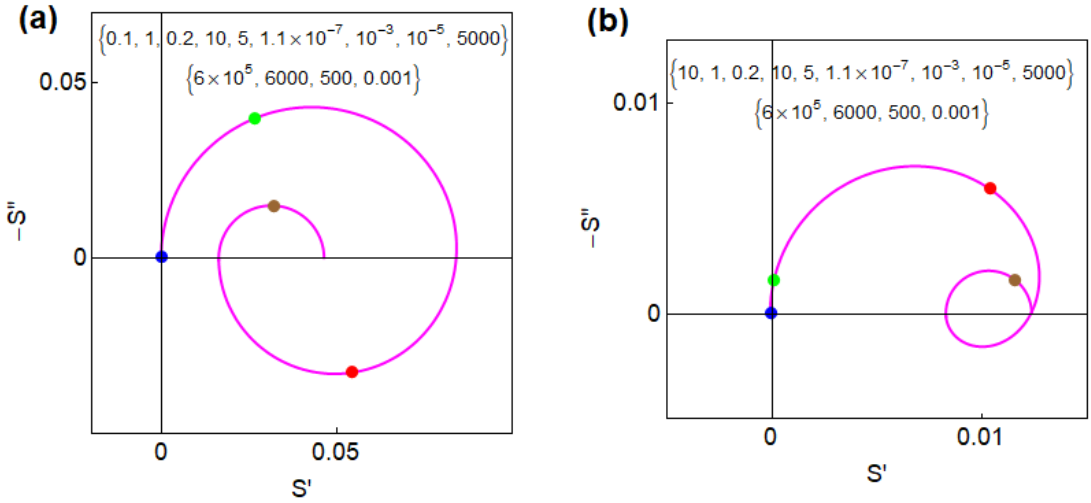

Figure S6. Simulation of the effect of the series resistance. Representation of transfer function S of voltage-modulated luminescence the complex plane. (a) $R_s = 0.1$, (b) $R_s = 10$. The parameters are indicated as $[R_s, R_{rad}, R_3, R_1, R_a, C_g, C_1, C_\mu, L_a]$ and $[\omega_\mu, \omega_h, \omega_d, \omega_a]$. $\varphi_{out} = 1$. The circuit elements have dimensionless values to illustrate the shape of spectra. The characteristic frequencies in Table 1 are indicated.

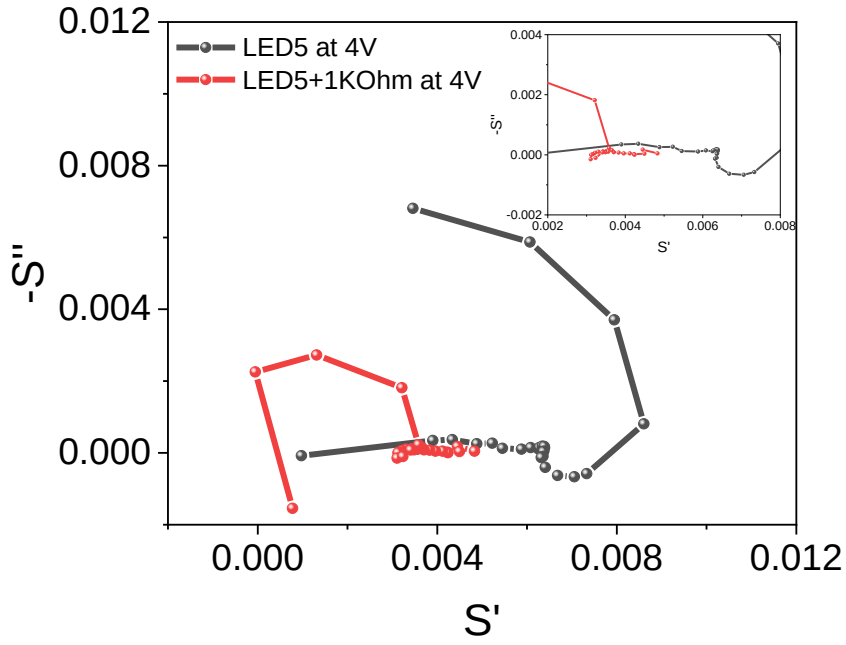

Figure S7. Measurement of the effect of the series resistance, by adding an external resistor of 1 kΩ to the LED5 device.

5. Experimental setup for LEVS data acquisition

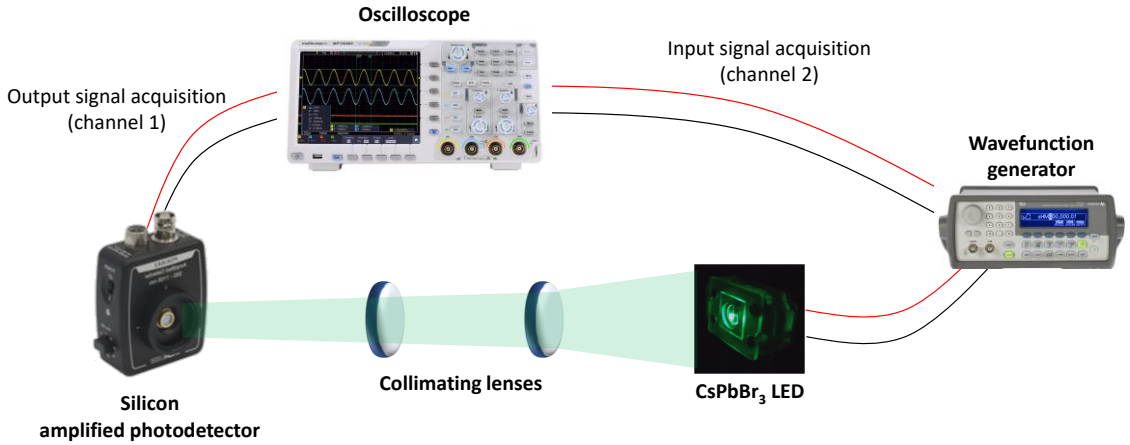

Figure S8. Illustration of the LEVS measuring setup.